of $CD3^+CD4^+HLA\text{-}DR^+$ cells, $CD3^+CD8^+HLA\text{-}DR^+$cells, $CD4^+CD25^+$ Tregs, $CD3^-CD16^-CD56^{high}$natural killer (NK) cells, and $CD3^-CD16^+CD56^{dim}$ NK cells. The frequencies of the immune subsets were analyzed by flow cytometry using FACS Canto-II (Becton Dickinson, NJ, USA).

ELISPOT assay

The detection of IFN-γ and IL-10 was performed using an ELISPOT Set (BD Biosciences, San Jose, CA, USA) according to the manufacturer's instructions. Cultures of PBMCs were established in triplicate on round-bottomed 96-well plates for all time points investigated, at a concentration of 3×10^5 cells per well in 100 µl RPMI 1640 containing 10 % fetal bovine serum (FBS). Positive spots were detected using an automated counting machine.

Detection of HBV-DNA and determination of HBV genotype

DNA was extracted from 100 µl of serum using SMITEST EX-R&D (Medical & Biological Laboratories, Nagoya, Japan) and dissolved in 20 µl of nuclease-free distilled water. The DNA preparation thus obtained (10 µl) was subjected to nested PCR with primers targeting the S gene of the HBV-DNA, as described previously [37]. Briefly, first-round PCR was carried out for 35 cycles (98 °C for 10 s, 55 °C for 15 s, and 72 °C for 1 min, with an additional 7 min in the last cycle) in the presence of PrimeSTAR HS DNA Polymerase (TaKaRa Bio, Shiga, Japan) and primers HB095 (sense, 5′-GAG TCT AGA CTC GTG GTG GAC-3′) and HB184 (antisense, 5′-CGA ACC ACT GAA CAA ATG GCA CCG-3′), for 25 cycles. This was followed by a second-round PCR consisting of 25 cycles using the same conditions as in the first round, with primers HB097 (sense, 5′-GAC TCG TGG TGG ACT TCT CTC-3′) and S2-2 (antisense, 5′-GGC ACT AGT AAA CTG AGC CA-3′). The HBV genotype was determined by phylogenetic analysis of the S gene sequence (437 nt) of the HBV isolates.

Detection of HCV RNA

RNAs were extracted from 250 µl of serum using TRIzol LS (Invitrogen, Tokyo, Japan). They were divided into two aliquots and each was assayed by reverse transcription (RT)-PCR with nested primers derived from the core region and NS5A interferon sensitivity determining region (ISDR) of the HCV genome. Nested PCR of the core region of the HCV genome was carried out with primers C008 (sense, 5′-AAC CTC AAA GAA AAA CCA AAC G-3′) and C011 (antisense, 5′-CAT GGG GTA CAT YCC GCT YG-3′) in the first round and C009 (sense, 5′-CCA CAG GAC GTY AAG TTC CC-3′) and C010 (antisense, 5′-AGG GTA TCG ATG ACC TTA CC-3′) in the second round. Nested primers that were derived from NS5A-ISDR of the HCV genomes were designed to amplify a 188-bp product with C004 (sense, 5′-ATG CCC ATG CCA GGT TCC AG-3′) and C005 (antisense, 5′-AGC TCC GCC AAG GCA GAA GA-3′) in the first round, and C006 (sense, 5′-ACC GG A TGT GGC AGT GCT CA-3′) and C007 (antisense, 5′-GTA ATC CGG GCG TGC CCA TA-3′) in the second round.

Analysis of nucleotide and amino acid sequences

The PCR products were sequenced directly on both strands using a BigDye Terminator version 3.1 Cycle Sequencing Kit on an ABI PRISM 3100 Genetic Analyzer (Applied Biosystems, Foster City, CA, USA). Sequence analysis was performed using Genetyx-Mac ver. 12.2.6 (Genetyx, Tokyo, Japan) and ODEN (version 1.1.1) from the DNA Data Bank of Japan (National Institute of Genetics, Mishima, Japan) [38]. Sequence alignments were generated using CLUSTAL W (Version 1.8) [39]. The phylogenetic tree was constructed by the neighbor-joining method [40]. The reliability of the phylogenetic results was assessed using 1000 bootstrap replicants [41]. The final tree was obtained with the Njplot program (version 2.2) [42].

Plasmid construction

HBV expression plasmids were constructed by previously published methods. Serum samples were obtained from two patients infected with HBV genotype Bj and two patients infected with HBV genotype C. HBV-DNA was extracted from 100 µl serum using a QIAamp DNA blood kit (QIAGEN, Hilden, Germany). Four primer sets were designed to amplify two fragments covering the entire HBV genome. Amplified fragments were inserted into a pGEM-T Easy Vector (Promega, Madison, WI, USA) and cloned in DH5a competent cells (TOYOBO, Osaka, Japan). Briefly, at least 5 clones of each fragment were sequenced and the consensus sequence was identified and used as a template for 1.24-fold the HBV genome of different genotypes (B1 indicates the genotype Bj35 clone; B2 indicates the genotype Bj56 clone; C1 indicates the genotype C-AT clone; and C2 indicates the genotype C-22 clone). The HCV-JFH-1 strain was provided by Dr. T. Wakita (National Institute of Infectious Diseases, Japan).

HCV and HBV expression in Huh 7 cells

Cell-culture-derived infectious HCV was generated as described previously [43]. The HCV was quantified as

follows: RNA was extracted from the Huh-7 culture supernatant using a QIAamp Viral RNA Kit (Qiagen, Valencia, CA, USA). The HCV RNA was quantified by real-time RT-PCR, using TaqMan EZ RT-PCR Core Reagents (Applied Biosystems) according to the manufacturer's protocol, using the published primers and probe [44]. The filtered (0.45 μm) culture supernatant of HCV-infected Huh-7 cells containing 2×10^8 HCV RNA copies/ml [equivalent to 9.7×10^4 focus-forming units (ffu)/ml] was used for the experiments. To analyze HCV-RNA in the supernatant, Huh-7 cells (2×10^5 cells in a 6-well plate) were infected with JFH-1 (multiplicity of infection [MOI] = 0.01) and after 4 h the cells were washed twice with phosphate-buffered saline (PBS). The supernatants were then collected and the cells were reseeded at 2×10^5 cells per 6-well plate. Then the HBV expression and mock plasmid were transfected by FuGENE6 (Roche Applied Science, IN, USA). The supernatant of the culture medium was collected 72 h after transfection. Quantification of HBV-DNA and HCV-RNA was carried out using real-time PCR.

IFN-α was added 24 h after the transfection of the HBV plasmids, and the supernatant of the culture medium was then collected 48 h after the addition of the IFN-α.

Results

Clinical characteristics of patients A and B

Patient A (high HBV-DNA titer and high HCV-RNA titer)

Patient A was a 44 year-old man with a high aspartate aminotransferase/alanine aminotransferase (AST/ALT) level. The prothrombin time-international normalized ratio (PT-INR) was in the normal range. Patient A had high HBV-DNA titers and high HCV-RNA titers (Table 1). His liver histology was classified as A2/F3 (Fig. 1). The laparoscopic analysis indicated moderate inflammation and intermediate fibrosis. The liver surfaces of the right lobe and left lobe were almost the same phenotype. Polymorphism of IL-28B (rs8099917) was T/G (hetero allele).

Patient B (low HBV-DNA titer and high HCV-RNA titer)

Patient B was a 63 year-old man with a low AST/ALT level. PT-INR was in the normal range. Patient B had low HBV-DNA titers and high HCV-RNA titers. The liver histology was classified as A2/F1 (Fig. 1). The liver surface showed moderate inflammation and was smooth. The polymorphism of IL-28B (rs8099917) was T/T (major homo allele).

Biopsy samples from patients with dual HBV and HCV infection were collected at the main liver centers in Miyagi prefecture. Fifteen HBV/HCV dual-infected patients were found in this study (Supplementary Table 1). Many of these patients had HCV-dominant infection and undetectable levels of HBV replication (10/15 patients). Most of the patients were HB envelope antigen (eAg)-negative and HBe antibody (Ab)-positive (14/14 patients). All HBV/HCV dual-infected patients who had received Peg-IFN-based

Table 1 Background of HBV/HCV dual-infected patients

	Patient A HCV high titer/ HBV high titer	Patient B HCV high titer/ HBV low titer	Normal range
Gender	Male	Male	
Age (years)	44	63	
HCV-RNA	6.5	5.5	log copies/ml
HCV genotype	1b	1b	
HBV-DNA	5.5	3.5	log copies/ml
HBV genotype	C	Bj	
HBe-Ag	129.5	0.5	0–0.9 index
HBe-Ab	0.1	99.3	0–49 %
Total bilirubin	0.7	1.2	0.2–1.2 mg/dl
Direct bilirubin	0.1	0.1	0–0.3 mg/dl
γ-GTP	208	31	8–57 IU/l
AST	138	33	12–30 IU/l
ALT	256	38	8–35 IU/l
Hb-A1c	5.3	5.4	4.3–5.8 %
Glu	103	83	68–106 mg/dl
BMI	25.34	18.75	
T-cho	160	195	128–220 mg/dl
LDL-cho	69	93	70–139 mg/dl
HDL-cho	37	67	36–89 md/dl
WBC	7800	5100	3200–9600/μl
RBC	491	446	428–566 × 10^4/μl
Hb	17.1	14.1	13.6–17.4 g/dl
PLT	169000	176000	155000–347000/μl
PT-INR	0.87	0.96	0–1.15 INR
Liver histology	A2/F3	A2/F1	METAVIR score
IL-28B SNP (rs8099917)	T/G	T/T	

HCV hepatitis C virus, *HBV* hepatitis B virus, e-*Ag* envelope antigen, *e-Ab* envelope antibody, *γ-GTP* γ-guanosine triphosphate, *AST* aspartate aminotransferase, *ALT* alanine aminotransferase, *Hb* hemoglobin, *Glu* glucose, *BMI* body mass index, *T-cho* total cholesterol, *LDL* low-density lipoprotein, *HDL* high-density lipoprotein, *PLT* platelets, *PT-INR* prothromin time-international normalized ratio, *IL* interleukin, *SNP* single-nucleotide polymorphism

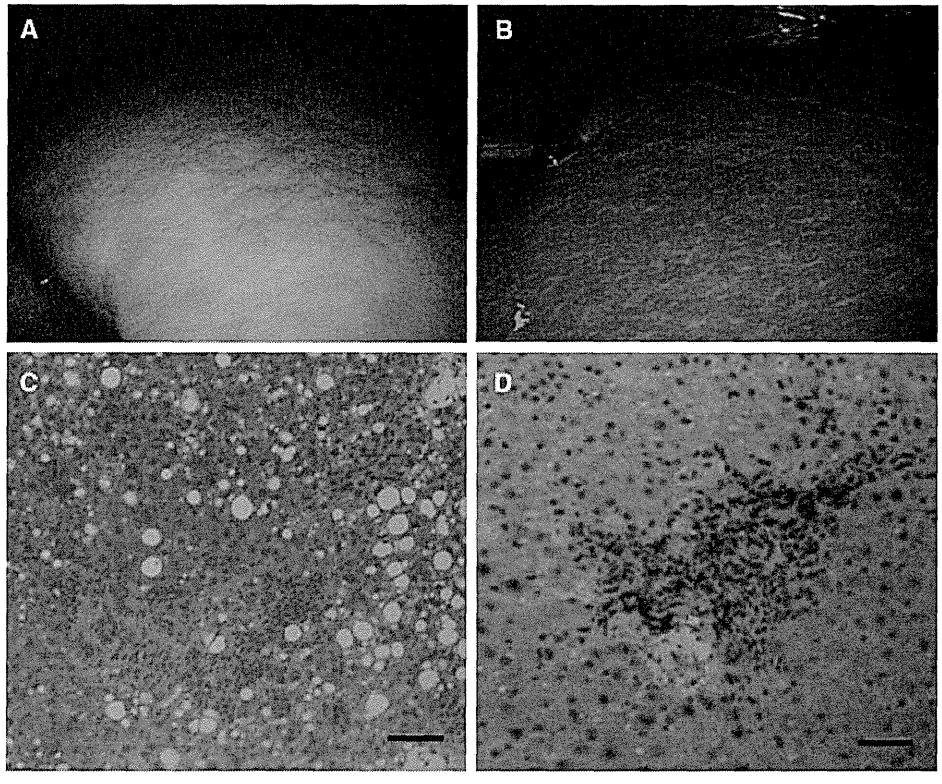

Fig. 1 Laparoscopic liver biopsy. The laparoscopic images of the liver surfaces of patient A (**a**) and patient B (**b**) are shown. Histopathology of patient A (**c**) and patient B (**d**) is also shown. *Bars* = 50 μm

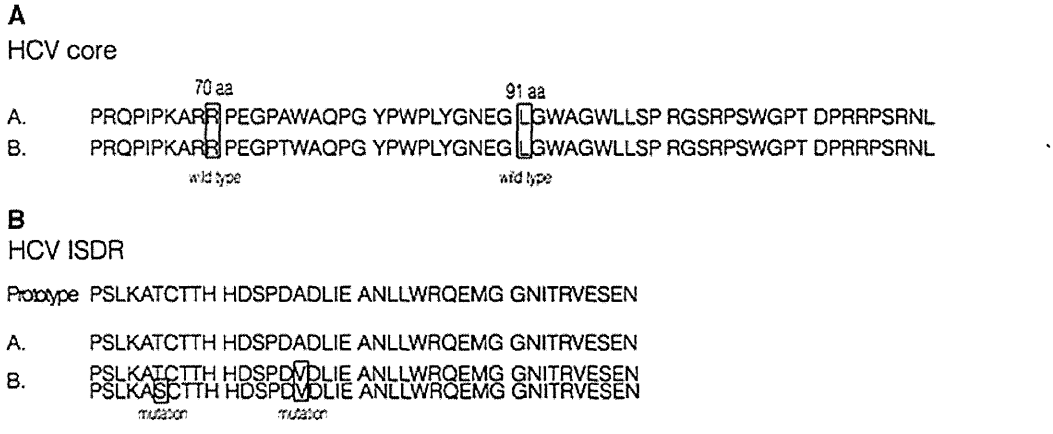

Fig. 2 Virological analysis of hepatitis B virus (HBV) and hepatitis C virus (HCV) in HBV/HCV dual infection. The amino acid sequences of the HCV-core region including core-70 and core-91, which were previously reported as determinants of the sensitivity to pegylated interferon/ribavirin (Peg-IFN/RBV) therapy, in patient A and patient B are shown (**a**). The amino acid sequences of the interferon sensitivity determining region (*ISDR*), which were previously reported as determinants of the sensitivity to IFN, in patients A and B are shown (**b**)

treatment achieved a sustained viral response (SVR) (5/5 patients). These data indicated that HCV-dominant dual-infected patients had good responses to treatment for HCV infection.

Virological analysis of HBV/HCV in patients A and B

The HCV genotype in both patient A and patient B was 1b. The sequences of amino acids in the ISDR region and HCV

core-70 and core-91 amino acids were analyzed by direct sequencing. Both patients had wild-type core-70 and core-91 amino acids (Fig. 2a). None of the mutations of the ISDR region was detected in patient A, but two of the mutations of the ISDR region were detected in patient B (Fig. 2b). The genotypes of HBV in patients A and B were analyzed by direct sequencing and phylogenetic tree analysis. The genotype of HBV in patient A was genotype C, which has been reported as difficult-to-treat HBV. The genotype of HBV in patient B was genotype Bj, which has been reported as easy-to-treat HBV in comparison to genotype C [45–47].

Sequential analysis of biochemical and virological data during Peg-IFN/RBV therapy

Patient A

In patient A, HCV-RNA gradually declined during Peg-IFN/RBV therapy. On the other hand, the HBV-DNA gradually increased during Peg-IFN/RBV therapy (Fig. 3a). The amount of HBeAg started to increase 9 months after the start of Peg-IFN/RBV therapy. HCV-RNA started to increase 12 months after the start of Peg-IFN/RBV therapy, although Peg-IFN/RBV was still being administered up to 18 months after the start of Peg-IFN/RBV therapy (Fig. 3a).

Patient B

In patient B, HCV-RNA and HBV-DNA rapidly declined after the start of Peg-IFN/RBV therapy (Fig. 3b). HCV-RNA could not be detected in peripheral blood 2 months after the start of Peg-IFN/RBV therapy. Peg-IFN/RBV was administered up to 12 months after the start of the Peg-IFN/RBV therapy. The amounts of HBeAb and HBeAg did not change during the Peg-IFN/RBV therapy (Fig. 3b).

Sequential immunological analysis during Peg-IFN/RBV therapy

We analyzed various subsets of immune cells that could affect the immunopathogenesis of HBV/HCV dual infection. NK cells ($CD3^-CD16^-CD56^{high}$ and $CD3^-CD16^+CD56^{dim}$) and NK-T cells ($CD3^+CD56^+CD16^+$, $CD3^+CD56^+CD16^-$ and $CD3^+CD56^-CD16^+$) were analyzed (Supplementary Fig. 1A). The $CD3^-$ gated lymphocytes were separated into 4 groups (a, b, c, and d). For these subsets, (a) indicated the presence of $CD3^-CD16^-CD56^{high}$ NK cells that could produce various cytokines vigorously and had low cytotoxic activity. Subset (b) showed $CD3^-CD16^+CD56^{dim}$ NK cells that had weak cytokine production ability and high cytotoxic activity.

The $CD3^+$ gated lymphocytes were separated into 3 groups (a, b, and c). The activated $CD3^+$, $CD3^+CD4^+$, and $CD3^+CD8^+$ T cells were analyzed (Supplementary Fig. 1B). $HLA\text{-}DR^+$ activated $CD3^+$, $CD3^+CD4^+$, and $CD3^+CD8^+$ T cells could be clearly distinguished by FACS analysis. Additionally, representative dot plots of Tregs and B cells were created (shown in Supplementary Fig. 1C). The frequencies of $CD3^-CD16^+CD56^{dim}$ NK cells, $CD3^+CD16^-CD56^+$ NK-T cells, activated $CD3^+CD4^+$ T cells, and activated $CD3^+CD8^+$ T cells fluctuated similarly during Peg-IFN/RBV therapy in patient A (Supplementary Fig. 1D). Activated T cells were increased at one month of Peg-IFN/RBV therapy, and the above subsets of lymphocytes gradually decreased up to 3 months of Peg-IFN/RBV therapy. After that, these cells gradually increased again up to 9 months of Peg-IFN/RBV therapy. In patient A, after 9 months of Peg-IFN/RBV therapy, these cells had decreased again (Supplementary Fig. 1D). The frequency of Tregs and activated B cells (data not shown) did not change during Peg-IFN/RBV therapy in patient A (Supplementary Fig. 1D). On the other hand, in patient B, the frequencies of $CD3^-CD16^+CD56^{dim}$ NK cells, $CD3^+CD16^-CD56^+$ NK-T cells, activated $CD3^+CD4^+$ T cells, and activated $CD3^+CD8^+$ T cells were increased and sustained during Peg-IFN/RBV therapy (Supplementary Fig. 1E). Five HCV monoinfected patients were analyzed by the same protocol (Supplementary Fig 1F). The mean frequency of various kinds of immune subsets was analyzed (Supplementary Fig 1F). The tendency of immunological reactions during Peg-IFN/RBV therapy in these five patients was similar to that in patient B.

Analysis of HBV- and HCV-specific immune responses

The analysis of HBV- and HCV-specific-immune responses was carried out by ELISPOT assay. Representative spots of IFN-γ are shown in Fig. 4a. In patient A, HCV- and HBV-specific IFN-γ secretion activities were remarkably low in comparison to the IL-10 secretion activity. Moreover, in patient A, the induction of IFN-γ-secreting cells could not be detected after Peg-IFN/RBV therapy, especially in regard to HBV-core specific IFN-γ secretion in PBMCs (Fig. 4b). On the other hand, in patient B, the HBV-core specific IFN-γ-secreting cells were high in comparison to those in patient A (Fig. 4c). Moreover, the induction of IFN-γ-secreting cells could be detected during Peg-IFN/RBV therapy in patient B (Fig. 4c). The mean numbers of IFN-γ- and IL-10-secreting spots in HBV-dominant dual-infected patients, patients with monoinfection with HBV genotype Bj ($HBeAb^+$), Bj ($HBeAg^+$), C ($HBeAb^+$), C ($HBeAg^+$), or HCV genotype 1b are shown in Fig. 4d. In patient A, HB core antigen (HBcAg)-specific IFN-γ secretion was weaker than that in

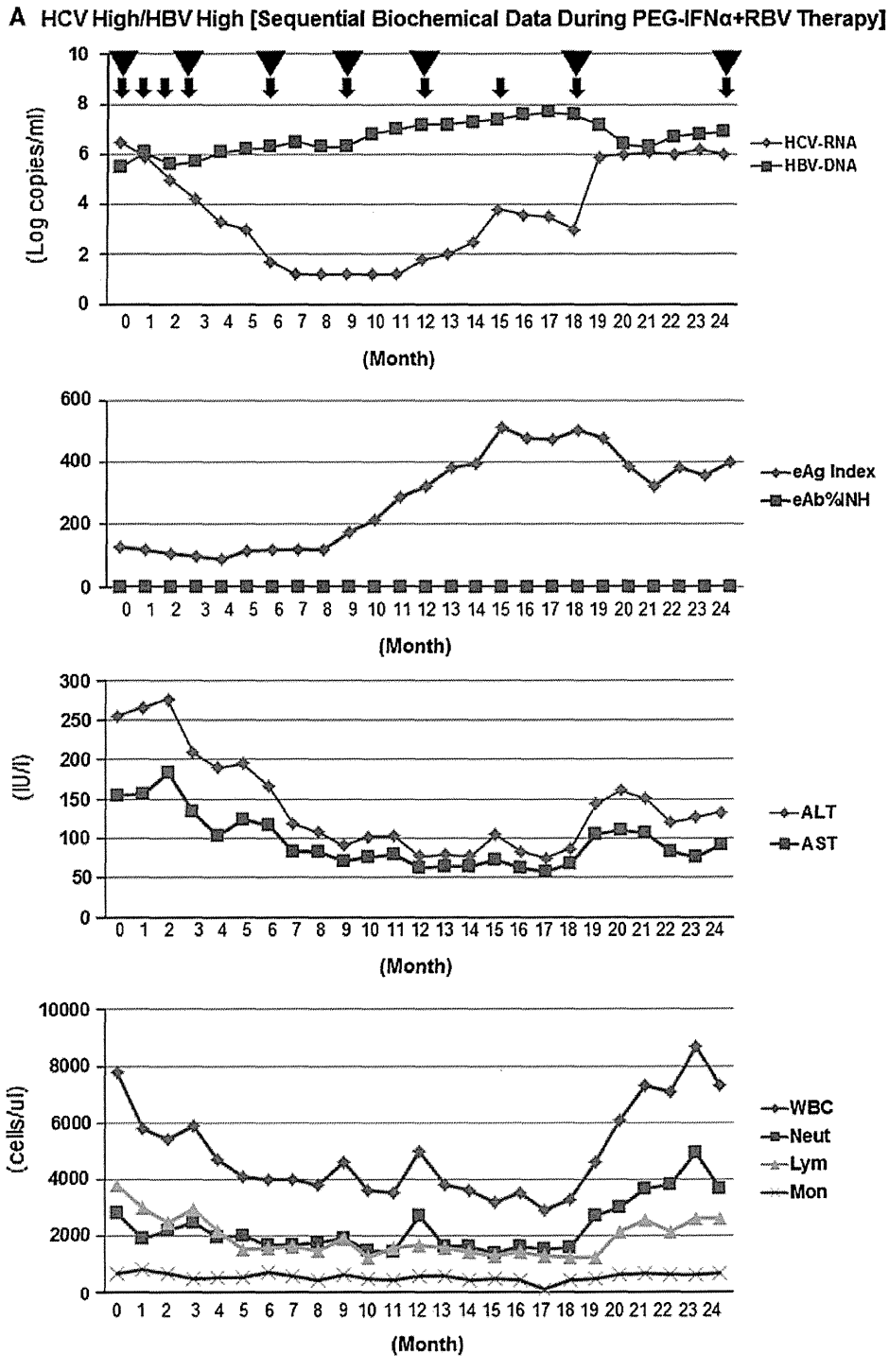

Fig. 3 Sequential biochemical data analysis during Peg-IFN/RBV therapy. The titers of HBV-DNA and HCV-RNA; the amounts of envelope antigen (*eAg*) and envelope antibody (*eAb*), and alanine aminotransferase (*ALT*) and aspartate aminotransferase (*AST*); and the numbers of WBCs, neutrophils (*Neut*), lymphocytes (*Lym*), and monocytes (*Mon*) in patients A (**a**) and B (**b**) are shown in these graphs. *Arrows* indicate the sampling points of FACS analysis. *Triangles* indicate the sampling points of the ELISPOT assay. *INH* inhibition

HBV-genotype C-monoinfected patients who were HBeAg-positive. However, HBcAg-specific IL-10 secretion in patient A was stronger than that in HBV-genotype C monoinfected patients who were HBeAg-positive. These data indicated that the presence of HCV might also suppress the HBV-specific immune response in regard to certain host factors (e.g., in the presence of IL-28B polymorphism, and depending on the body mass index [BMI] and γ-guanosine triphosphate [γ-GTP] level), because the presence of HCV did not suppress the HBV-specific immune response either in patient B or in the patients with dual HCV-dominant infection. Otherwise, we could deny the possibility indicating that

Fig. 3 continued

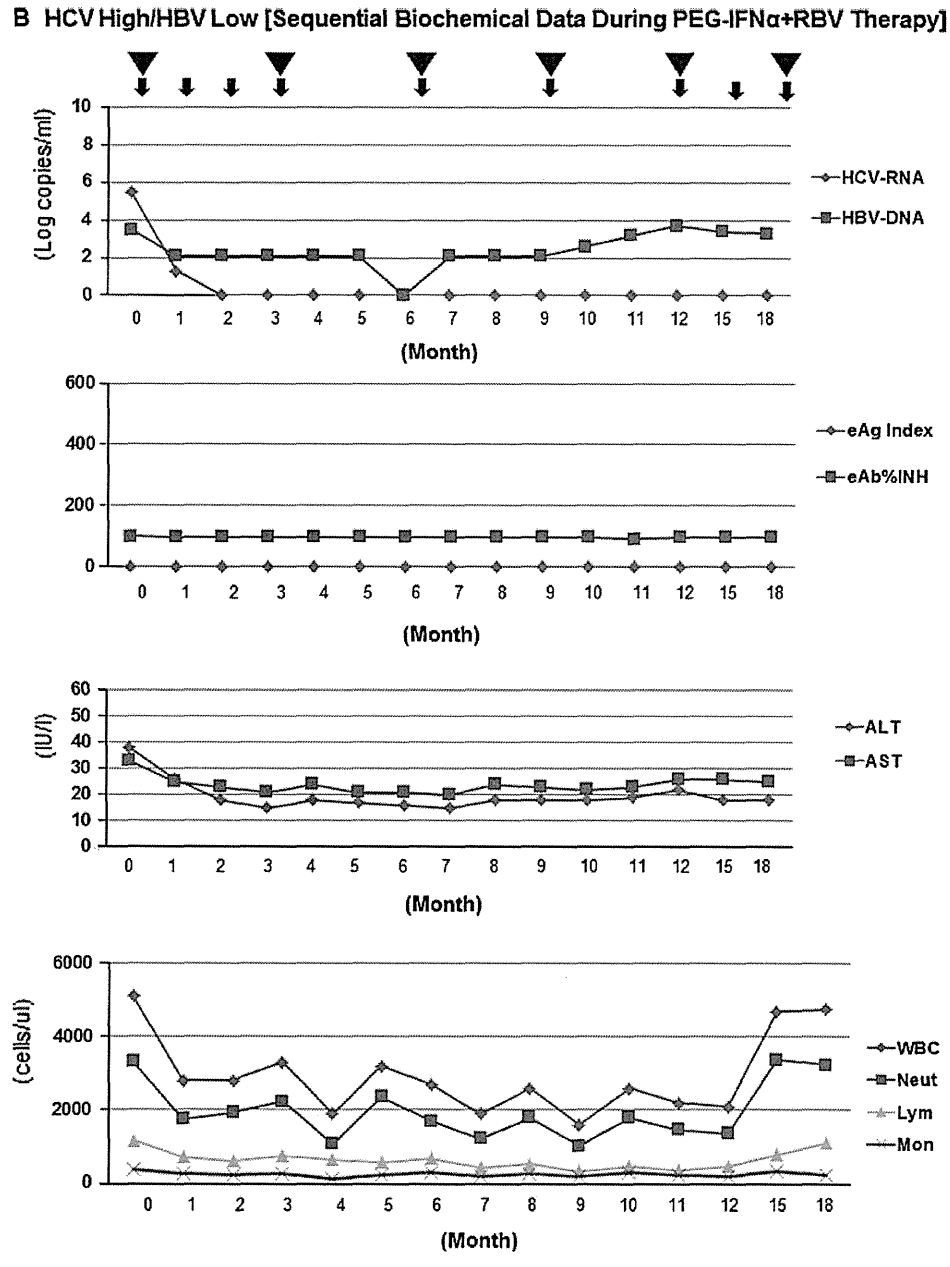

the certain background of host factors could allow the existence of dual virus actively. These data indicated that HBV-specific IL-10-secreting cells and/or certain kinds of host factors had an important role in HBV- and HCV-specific immune suppression in patient A, but not in patient B.

In vitro analysis of HBV/HCV dual infection

We carried out in vitro analysis of HBV/HCV infection using Huh-7 cells that were susceptible to the HCV-JFH-1 strain and HBV expression plasmids. The amount of the JFH-1 strain did not change with the various kinds of HBV expression plasmids (Fig. 5a). Moreover, the amounts of the various HBV strains did not change in the presence of JFH-1 infection. These data indicated that no direct effect of HBV and HCV could be detected in Huh 7 cells. We carried out experiments to analyze the effect of IFN-α treatment on HCV Huh-7 cells with various kinds of HBV expression (Fig. 5b). In our systems, it appeared that HBV expression could not significantly affect the suppressive effect of IFN-α.

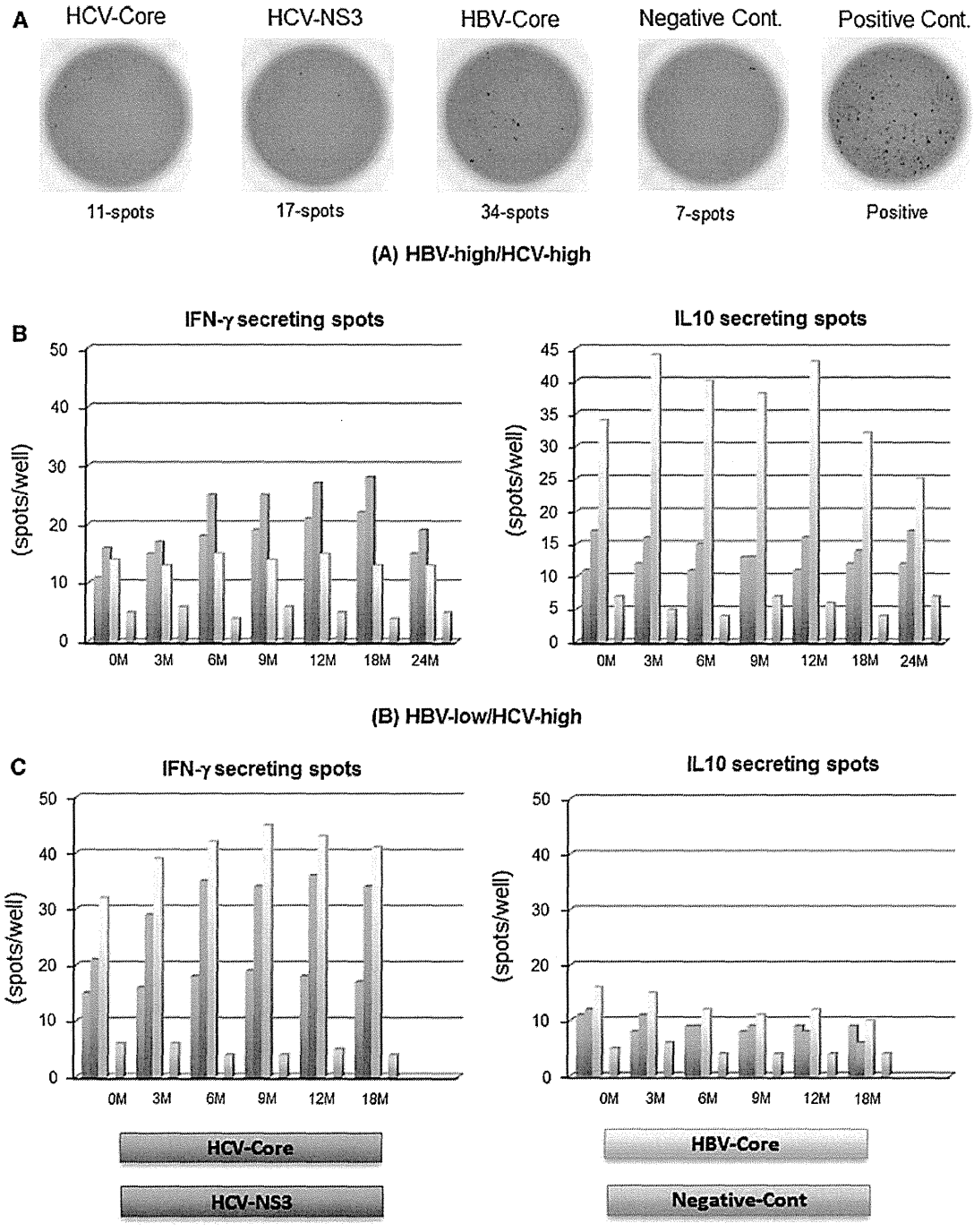

Fig. 4 The sequential analysis of HBV/HCV-specific immune reactions during Peg-IFN/RBV therapy. Representative spots of the ELISPOT assay are shown (**a**). The sequential data of IFN-γ- and interleukin-10 (*IL-10*)- secreting spots in patient A are shown (**b**). The sequential data of IFN-γ- and IL-10-secreting spots in patient B are shown (**c**). Comparison of IFN-γ- and IL-10- secreting spots in patient A before starting therapy, patient B before starting therapy, dual HCV-dominant patients, HCV-monoinfected patients, HBV-Bj ($HBeAb^+$) monoinfected patients, HBV-Bj ($HBeAg^+$) monoinfected patients, HBV-C ($HBeAb^+$) monoinfected patients, and HBV-C ($HBeAg^+$) monoinfected patients (**d**). In these *bar graphs*, the *blue bars* indicate HCV-core specific reaction. The *red bars* indicate HCV-NS3 specific reaction. The *green bars* indicate HBV-core specific reaction. The *aqua blue bars* indicate the negative control (*Cont.*). *Error bars* indicate standard deviations (color figure online)

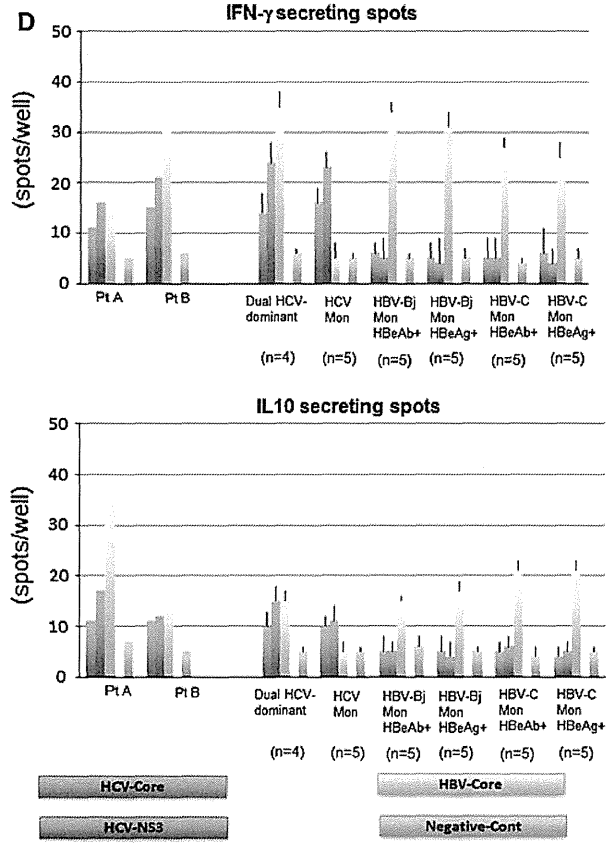

Fig. 4 continued

Discussion

The immunopathogenesis of dual hepatitis B and C infection is not clear, given the complexity of viral and host factors [19, 21, 48–50]. However, detailed understanding of specific patients with dual hepatitis B and C infection could contribute to improving the treatment and follow up of these patients. Therefore, we focused on two representative patients with HBV/HCV dual infection who received Peg-IFN/RBV therapy.

Concerning the virological results, patient A had genotype 1b, HCV-Core 70 wild-type and low mutation of ISDR HCV and genotype C HBV. It has been reported that genotype 1b HCV is common in Japan and is usually difficult to treat in comparison to genotypes 2a and 2b [51]. Among genotype 1b HCV strains, HCV-Core 70 wild-type HCV is easily decreased by Peg-IFN/RBV therapy [51]. On the other hand, it has been reported that in genotype 1b HCV low mutation of ISDR is difficult to treat [52]. Patient B had almost the same background of HCV–genotype 1b, HCV-Core 70 wild-type, and low mutation of ISDR–as patient A. However, the background of host factors that could affect the responsiveness of IFN-based therapy was different between patients A and B. For example, patient A had a hetero allele of the IL-28B polymorphism, advanced fibrosis, and fatty changes of the liver. On the other hand, patient B had the major allele of the IL-28B polymorphism and mild fibrosis. Moreover, the background of HBV in patient B was completely different from that in patient A. It has been reported that HBV genotype Bj is usually more susceptible to IFN-based therapy than genotype C [45, 53]. Therefore, not only the HBV factors but also the combination of host factors and HBV factors might affect the responsiveness to IFN-based therapy. In patient A, the responsiveness of HCV during Peg-IFN/RBV therapy was relatively poor. However, the viral titers of HCV were lower than 1.2 log copies/ml at 7 months after the start of therapy. During the reduction of the HCV viral titers, the titers of HBV and HBc-Ag specific IL-10-secreting cells were gradually increased. Although patient A had received Peg-IFN/RBV therapy for up to 18 months, HCV-RNA increased again 12 months after the start of the therapy. The sustained Th1 immune suppression might have contributed to the relapse of HCV. Not only weak up-regulation of HCV-specific Th1 immune reaction but also strong up-regulation of HBV-specific IL-10-secreting activity was detected during Peg-IFN/RBV therapy in patient A [26, 35]. Moreover, increased HBeAg could be detected 9 months after the start of the therapy. Fluctuations of activated CD4 cells, CD8 cells, NK cells, and NK-T cells could be seen in patient A. On the other hand, in patient B, the responsiveness of HBV and HCV during Peg-IFN/RBV therapy was good. Moreover, the immune response of patient B was almost comparable to the responses in the patients with HCV monoinfection and those with HBV-genotype Bj monoinfection. Previously, it has been reported that Peg-IFN/RBV therapy could achieve almost the same SVR rates in patients with HCV/HBV dual infection and those with HCV monoinfection [54–56]. We assume that the results in these studies were obtained from patients similar to our patient B, because the number of patients with HCV-dominant infection is much higher than the number of those with HBV/HCV dual active infection such as our patient A. Patients with HBV/HCV dual active infection such as patient A are relatively rare in Japan. However, it is necessary to understand the immunopathogenesis of these patients, because Peg-IFN/RBV therapy might not be sufficient to eradicate or control HBV/HCV in these difficult-to-treat patients. One of the candidate therapies for such patients might be Entecavir (ETV)/Peg-IFN/RBV sequential therapy. The effect of HBV specific regulatory T cells might contribute to the immunosuppression of not only HBV but also HCV [35]. In some previous studies, including ours, it has been reported that HBV replication might contribute to immune suppression [19, 29].

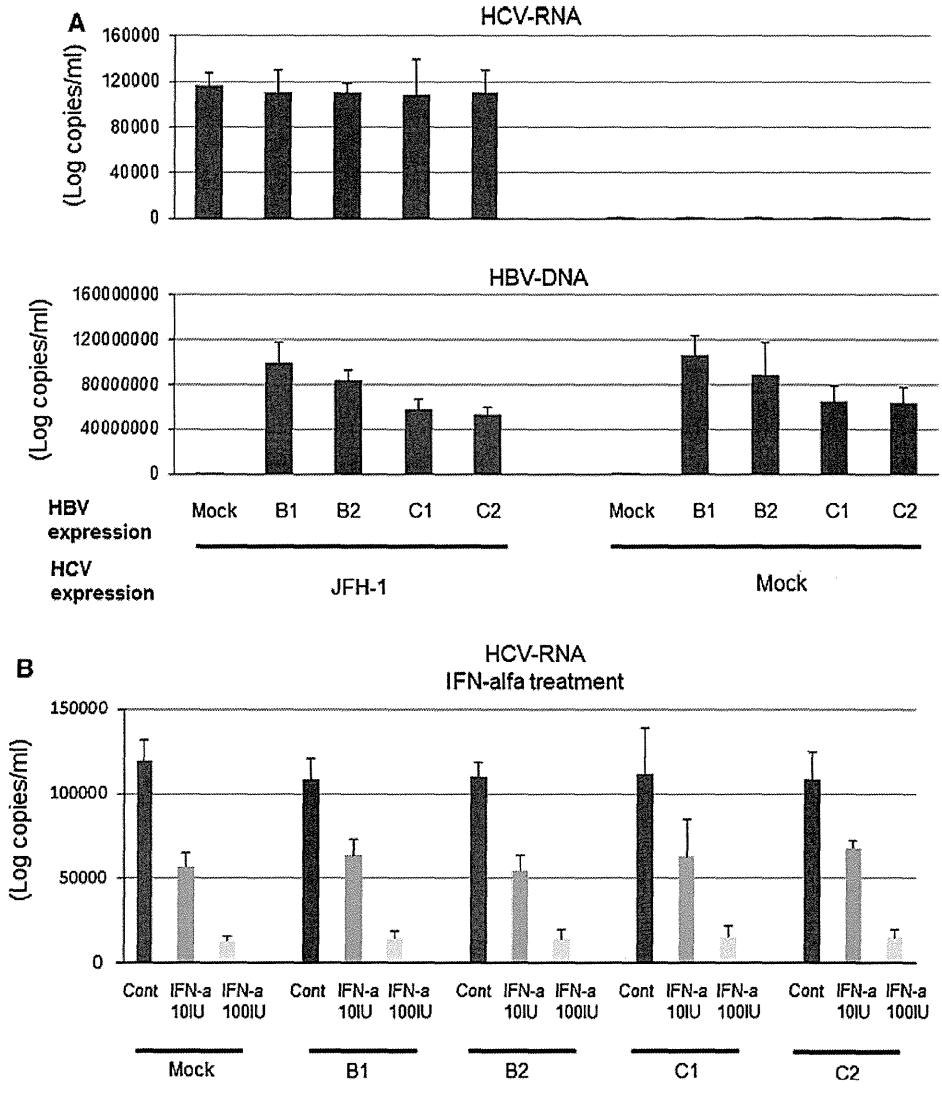

Fig. 5 In vitro analysis of HBV/HCV dual infection. The titers of HCV-RNA and HBV-DNA are shown. *B1* indicates genotype Bj35 clone. *B2* indicates genotype Bj56 clone. *C1* indicates genotype C-AT clone. *C2* indicates genotype C-22 clone (**a**). The titers of HCV-RNA after the IFN-α treatment are shown (**b**)

In the present study, we employed an in vitro coinfection system to analyze the direct interaction between HBV and HCV. In our system, we used several different HBV clones, because it is necessary to consider the effects of different genotypes. Although we could not detect the direct interaction of HBV/HCV in our system, we could not exclude the possibility of indirect interaction between cytokines and chemokines produced from virus-infected hepatocytes. We are now analyzing the chemokines produced from hepatoma cells with different HBV genotype clones (ongoing study).

In conclusion, we analyzed data from representative patients with HBV/HCV dual infection sequentially and precisely. Because many different kinds of backgrounds might affect immunoreactions, we focused on representative patients and analyzed the immunological responses extensively. There might be a group of patients with very difficult-to-treat dual infections. We need to understand the immunopathogenesis of such patients to develop the appropriate therapy.

Acknowledgments This work was supported in part by a Grant-in Aid from the Ministry of Education, Culture, Sport, Science, and Technology of Japan (Y.K. #23790761), and grants from the Ministry of Health, Labor, and Welfare of Japan.

Conflict of interest The authors declare that they have no conflict of interest.

References

1. Alter MJ, Kruszon-Moran D, Nainan OV, et al. The prevalence of hepatitis C virus infection in the United States, 1988 through 1994. N Engl J Med. 1999;341(8):556–62.

2. Tiollais P, Pourcel C, Dejean A. The hepatitis B virus. Nature. 1985;317(6037):489–95.
3. Lai CL, Ratziu V, Yuen MF, Poynard T. Viral hepatitis B. Lancet. 2003;362(9401):2089–94.
4. Poynard T, Yuen MF, Ratziu V, Lai CL. Viral hepatitis C. Lancet. 2003;362(9401):2095–100.
5. Potthoff A, Manns MP, Wedemeyer H. Treatment of HBV/HCV coinfection. Expert Opin Pharmacother. 2010;11(6):919–28.
6. Chu CJ, Lee SD. Hepatitis B virus/hepatitis C virus coinfection: epidemiology, clinical features, viral interactions and treatment. J Gastroenterol Hepatol. 2008;23(4):512–20.
7. Bini EJ, Perumalswami PV. Hepatitis B virus infection among American patients with chronic hepatitis C virus infection: prevalence, racial/ethnic differences, and viral interactions. Hepatology. 2010;51(3):759–66.
8. Halima SB, Bahri O, Maamouri N, et al. Serological and molecular expression of hepatitis B infection in patients with chronic hepatitis C from Tunisia, North Africa. Virol J. 2010;7:229.
9. Saravanan S, Velu V, Nandakumar S, et al. Hepatitis B virus and hepatitis C virus dual infection among patients with chronic liver disease. J Microbiol Immunol Infect. 2009;42(2):122–8.
10. Lee LP, Dai CY, Chuang WL, et al. Comparison of liver histopathology between chronic hepatitis C patients and chronic hepatitis B and C-coinfected patients. J Gastroenterol Hepatol. 2007;22(4):515–7.
11. Liu Z, Hou J. Hepatitis B virus (HBV) and hepatitis C virus (HCV) dual infection. Int J Med Sci. 2006;3(2):57–62.
12. Tsai JF, Jeng JE, Ho MS, et al. Effect of hepatitis C and B virus infection on risk of hepatocellular carcinoma: a prospective study. Br J Cancer. 1997;76(7):968–74.
13. Cho LY, Yang JJ, Ko KP, et al. Coinfection of hepatitis B and C viruses and risk of hepatocellular carcinoma: systematic review and meta-analysis. Int J Cancer. 2011;128(1):176–84.
14. Huo TI, Huang YH, Hsia CY, et al. Characteristics and outcome of patients with dual hepatitis B and C-associated hepatocellular carcinoma: are they different from patients with single virus infection? Liver Int. 2009;29(5):767–73.
15. Kew MC. Interaction between hepatitis B and C viruses in hepatocellular carcinogenesis. J Viral Hepat. 2006;13(3):145–9.
16. Liu CJ, Chen PJ, Chen DS. Dual chronic hepatitis B virus and hepatitis C virus infection. Hepatol Int. 2009;3(4):517–25.
17. Bellecave P, Gouttenoire J, Gajer M, et al. Hepatitis B and C virus coinfection: a novel model system reveals the absence of direct viral interference. Hepatology. 2009;50(1):46–55.
18. Eyre NS, Phillips RJ, Bowden S, et al. Hepatitis B virus and hepatitis C virus interaction in Huh-7 cells. J Hepatol. 2009;51(3):446–57.
19. Chisari FV, Ferrari C. Hepatitis B virus immunopathogenesis. Annu Rev Immunol. 1995;13:29–60.
20. Koziel MJ. The role of immune responses in the pathogenesis of hepatitis C virus infection. J Viral Hepat. 1997;4(Suppl 2):31–41.
21. Rice CM, Walker CM. Hepatitis C virus-specific T lymphocyte responses. Curr Opin Immunol. 1995;7(4):532–8.
22. Nan XP, Zhang Y, Yu HT, et al. Circulating $CD4^{+}CD25^{high}$ regulatory T cells and expression of PD-1 and BTLA on $CD4^{+}$ T cells in patients with chronic hepatitis B virus infection. Viral Immunol. 2010;23(1):63–70.
23. Kondo Y, Ueno Y, Shimosegawa T. Immunopathogenesis of hepatitis B persistent infection: implications for immunotherapeutic strategies. Clin J Gastroenterol. 2009;2(2):71–9.
24. Peng G, Li S, Wu W, Sun Z, Chen Y, Chen Z. Circulating $CD4^{+}$ $CD25^{+}$ regulatory T cells correlate with chronic hepatitis B infection. Immunology. 2008;123(1):57–65.
25. Maier H, Isogawa M, Freeman GJ, Chisari FV. PD-1:PD-L1 interactions contribute to the functional suppression of virus-specific $CD8^{+}$ T lymphocytes in the liver. J Immunol. 2007;178(5):2714–20.
26. Kondo Y, Kobayashi K, Ueno Y, et al. Mechanism of T cell hyporesponsiveness to HBcAg is associated with regulatory T cells in chronic hepatitis B. World J Gastroenterol. 2006;12(27):4310–7.
27. Stoop JN, van der Molen RG, Baan CC, et al. Regulatory T cells contribute to the impaired immune response in patients with chronic hepatitis B virus infection. Hepatology. 2005;41(4):771–8.
28. Kondo Y, Kobayashi K, Asabe S, et al. Vigorous response of cytotoxic T lymphocytes associated with systemic activation of CD8 T lymphocytes in fulminant hepatitis B. Liver Int. 2004;24(6):561–7.
29. Kondo Y, Asabe S, Kobayashi K, et al. Recovery of functional cytotoxic T lymphocytes during lamivudine therapy by acquiring multi-specificity. J Med Virol. 2004;74(3):425–33.
30. Kondo Y, Ueno Y, Kakazu E, et al. Lymphotropic HCV strain can infect human primary naive CD4(+) cells and affect their proliferation and IFN-gamma secretion activity. J Gastroenterol. 2011;46:232–41.
31. Kondo Y, Machida K, Liu HM, et al. Hepatitis C virus infection of T cells inhibits proliferation and enhances fas-mediated apoptosis by down-regulating the expression of CD44 splicing variant 6. J Infect Dis. 2009;199(5):726–36.
32. Kondo Y, Sung VM, Machida K, Liu M, Lai MM. Hepatitis C virus infects T cells and affects interferon-gamma signaling in T cell lines. Virology. 2007;361(1):161–73.
33. Ulsenheimer A, Gerlach JT, Gruener NH, et al. Detection of functionally altered hepatitis C virus-specific CD4 T cells in acute and chronic hepatitis C. Hepatology. 2003;37(5):1189–98.
34. Cramp ME, Rossol S, Chokshi S, Carucci P, Williams R, Naoumov NV. Hepatitis C virus-specific T-cell reactivity during interferon and ribavirin treatment in chronic hepatitis C. Gastroenterology. 2000;118(2):346–55.
35. Kondo Y, Ueno Y, Kobayashi K, et al. Hepatitis B virus replication could enhance regulatory T cell activity by producing soluble heat shock protein 60 from hepatocytes. J Infect Dis. 2010;202(2):202–13.
36. Nguyen LH, Ko S, Wong SS, et al. Ethnic differences in viral dominance patterns in patients with hepatitis B virus and hepatitis C virus dual infection. Hepatology. 2011;53(6):1839–45.
37. Takahashi M, Nishizawa T, Gotanda Y, et al. High prevalence of antibodies to hepatitis A and E viruses and viremia of hepatitis B, C, and D viruses among apparently healthy populations in Mongolia. Clin Diagn Lab Immunol. 2004;11(2):392–8.
38. Ina Y. ODEN: a program package for molecular evolutionary analysis and database search of DNA and amino acid sequences. Comput Appl Biosci. 1994;10(1):11–2.
39. Thompson JD, Higgins DG, Gibson TJ. CLUSTAL W: improving the sensitivity of progressive multiple sequence alignment through sequence weighting, position-specific gap penalties and weight matrix choice. Nucleic Acids Res. 1994;22(22):4673–80.
40. Saitou N, Nei M. The neighbor-joining method: a new method for reconstructing phylogenetic trees. Mol Biol Evol. 1987;4(4):406–25.
41. Felsenstein J. Estimating effective population size from samples of sequences: a bootstrap Monte Carlo integration method. Genet Res. 1992;60(3):209–20.
42. Perriere G, Gouy M. WWW-query: an on-line retrieval system for biological sequence banks. Biochimie. 1996;78(5):364–9.
43. Wakita T, Pietschmann T, Kato T, et al. Production of infectious hepatitis C virus in tissue culture from a cloned viral genome. Nat Med. 2005;11(7):791–6.
44. Takeuchi T, Katsume A, Tanaka T, et al. Real-time detection system for quantification of hepatitis C virus genome. Gastroenterology. 1999;116(3):636–42.

45. Sugauchi F, Kumada H, Sakugawa H, et al. Two subtypes of genotype B (Ba and Bj) of hepatitis B virus in Japan. Clin Infect Dis. 2004;38(9):1222–8.
46. Sugauchi F, Orito E, Ichida T, et al. Epidemiologic and virologic characteristics of hepatitis B virus genotype B having the recombination with genotype C. Gastroenterology. 2003; 124(4):925–32.
47. Orito E, Mizokami M, Sakugawa H, et al. A case–control study for clinical and molecular biological differences between hepatitis B viruses of genotypes B and C. Japan HBV Genotype Research Group. Hepatology. 2001;33(1):218–23.
48. Raimondo G, Brunetto MR, Pontisso P, et al. Longitudinal evaluation reveals a complex spectrum of virological profiles in hepatitis B virus/hepatitis C virus-coinfected patients. Hepatology. 2006;43(1):100–7.
49. Chuang WL, Dai CY, Chang WY, et al. Viral interaction and responses in chronic hepatitis C and B coinfected patients with interferon-alpha plus ribavirin combination therapy. Antivir Ther. 2005;10(1):125–33.
50. Tsai SL, Liaw YF, Yeh CT, Chu CM, Kuo GC. Cellular immune responses in patients with dual infection of hepatitis B and C viruses: dominant role of hepatitis C virus. Hepatology. 1995;21(4):908–12.
51. Akuta N, Suzuki F, Hirakawa M, et al. Amino acid substitution in hepatitis C virus core region and genetic variation near the interleukin 28B gene predict viral response to telaprevir with peginterferon and ribavirin. Hepatology. 2010;52(2):421–9.
52. Fukuma T, Enomoto N, Marumo F, Sato C. Mutations in the interferon-sensitivity determining region of hepatitis C virus and transcriptional activity of the nonstructural region 5A protein. Hepatology. 1998;28(4):1147–53.
53. Akuta N, Kumada H. Influence of hepatitis B virus genotypes on the response to antiviral therapies. J Antimicrob Chemother. 2005;55(2):139–42.
54. Yu ML, Lee CM, Chuang WL, et al. HBsAg profiles in patients receiving peginterferon alfa-2a plus ribavirin for the treatment of dual chronic infection with hepatitis B and C viruses. J Infect Dis. 2010;202(1):86–92.
55. Yu JW, Sun LJ, Zhao YH, Kang P, Gao J, Li SC. Analysis of the efficacy of treatment with peginterferon alpha-2a and ribavirin in patients coinfected with hepatitis B virus and hepatitis C virus. Liver Int. 2009;29(10):1485–93.
56. Liu CJ, Chuang WL, Lee CM, et al. Peginterferon alfa-2a plus ribavirin for the treatment of dual chronic infection with hepatitis B and C viruses. Gastroenterology. 2009;136((2)):496.e3–504.e3.